Magnetic Resonance Letters 6 (2026) 200222

Contents lists available at ScienceDirect

Magnetic Resonance Letters

journal homepage: www.keaipublishing.com/MRL

Research Article

Protamine-1 encoded recombinant adeno-associated virus for enhanced brain magnetic resonance imaging

Kairu Xie [a], Yaping Yuan [a,b], Mou Jiang [a], Daiqin Chen [a,b], Shizhen Chen [a,b,*], Xin Zhou [a,b,c,**]

[a] State Key Laboratory of Magnetic Resonance Spectroscopy and Imaging, National Center for Magnetic Resonance in Wuhan, Wuhan Institute of Physics and Mathematics, Innovation Academy for Precision Measurement Science and Technology, Chinese Academy of Sciences-Wuhan National Laboratory for Optoelectronics, Huazhong University of Science and Technology, Wuhan, 430071, China
[b] University of Chinese Academy of Sciences, Beijing, 100049, China
[c] Key Laboratory of Biomedical Engineering of Hainan Province, School of Biomedical Engineering, Hainan University, Haikou, 570228, China

ARTICLE INFO

Article history:
Received 13 March 2025
Received in revised form 27 April 2025
Accepted 3 June 2025
Available online 18 June 2025

Keywords:
Magnetic resonance imaging (MRI)
Chemical exchange saturation transfer (CEST)
Protamine 1 (PRM1)
Recombinant adeno-associated virus (rAAVs)

ABSTRACT

Magnetic resonance imaging (MRI) is a powerful tool for diagnosing and monitoring brain diseases, but its low sensitivity can hinder early detection. To address this challenge, we utilized chemical exchange saturation transfer (CEST) MRI, which greatly enhances sensitivity for detecting low-concentration compounds. In this study, we developed a CEST contrast agent based on a recombinant adeno-associated viruses (rAAVs) encoding the protamine-1 (PRM1) MRI reporter gene. CEST MRI revealed that PRM1 contrast agent effectively highlighted caudate putamen region after injection of the rAAVs into the mouse brain, clearly distinguishing it from the surrounding tissue, with no observable damage. This method provides a sensitive, metal-free CEST contrast agent for *in vivo* brain cell detection, demonstrating potential for both diagnostic and therapeutic applications in brain diseases.

© 2025 The Authors. Publishing services by Elsevier B.V. on behalf of KeAi Communications Co. Ltd. This is an open access article under the CC BY-NC-ND license (http://creativecommons.org/licenses/by-nc-nd/4.0/).

1. Introduction

Magnetic resonance imaging (MRI) is a highly practical technique for soft tissue imaging with superior spatial and temporal resolution, making it particularly valuable for diagnosing and monitoring brain diseases [1,2]. However, the relatively low sensitivity of MRI can pose challenges for early diagnosis and precise monitoring in clinical settings. This limitation can be addressed by increasing magnetic field strength, utilizing contrast agents, or adopting novel imaging

* Corresponding author. State Key Laboratory of Magnetic Resonance Spectroscopy and Imaging, National Center for Magnetic Resonance in Wuhan, Wuhan Institute of Physics and Mathematics, Innovation Academy for Precision Measurement Science and Technology, Chinese Academy of Sciences-Wuhan National Laboratory for Optoelectronics, Huazhong University of Science and Technology, Wuhan, 430071, China.
** Corresponding author. State Key Laboratory of Magnetic Resonance Spectroscopy and Imaging, National Center for Magnetic Resonance in Wuhan, Wuhan Institute of Physics and Mathematics, Innovation Academy for Precision Measurement Science and Technology, Chinese Academy of Sciences-Wuhan National Laboratory for Optoelectronics, Huazhong University of Science and Technology, Wuhan, 430071, China.
E-mail addresses: chenshizhen@wipm.ac.cn (S. Chen), xinzhou@wipm.ac.cn (X. Zhou).
Peer review under the responsibility of Innovation Academy for Precision Measurement Science and Technology (APM), CAS.

https://doi.org/10.1016/j.mrl.2025.200222
2772-5162/© 2025 The Authors. Publishing services by Elsevier B.V. on behalf of KeAi Communications Co. Ltd. This is an open access article under the CC BY-NC-ND license (http://creativecommons.org/licenses/by-nc-nd/4.0/).

techniques [3–5]. The widely utilized gadolinium-based contrast agents may enhance MRI signals by shortening the longitudinal relaxation time (T_1) of hydrogen nuclei (^{1}H) in lesion areas [6,7]. However, they are diffused uniformly throughout the extracellular space when intravenously administered due to their poor selectivity, posing high risks of toxicity and deposition in the brain [8,9].

Chemical exchange saturation transfer (CEST) MRI indirectly detects native molecules without labeling by manipulating the water proton signal through selective saturation of exchangeable protons. CEST method provides an effective sensitivity enhancement mechanism, allowing the visualization of low-concentration solutes via the water signal [10,11]. Recent researches have identified several effective CEST agents, including glucose [12,13], myo-inositol [14], glutamate [15], and creatine [16,17]. However, imaging endogenous substances in living organisms often suffers from poor specificity due to background signal interference. To overcome this limitation, exogenous agents not naturally present in the brain can be introduced. For example, protamine-1 (PRM1), primarily found in male germ cells, has been proposed as a potential CEST contrast agent due to its high concentration of guanidine-based protons, which can exchange with water protons [18].

Recombinant adeno-associated viruses (rAAVs) vectors are intensively used for delivering exogenous genes in brain research due to their excellent transfection efficacy and low cytotoxicity [19]. Utilizing MRI contrast agents encoded by rAAVs can further enhance the utility of MRI in brain imaging [20,21]. For instance, rAAVs can encode aquaporins, which selectively enhance water diffusivity in neurons, thus enabling diffusion-weighted MRI [22].

Herein, we proposed a novel methodology for *in vivo* brain-enhanced MRI. After demonstrating the CEST properties of PRM1 in solution, we transfected 293T cells with a plasmid expressing PRM1 and subjected them to CEST MRI analysis. Additionally, we established a recombinant adeno-associated virus 2 (rAAV2) delivery system encoding PRM1 and injected it into the caudate putamen (CPU) region of the mouse brain. Thirty days post-injection, CEST MRI was performed to assess the targeted CPU region (See Graphical abstract). This approach offers a promising approach for detecting specific brain cell types in live animals, providing valuable insights into dynamic brain changes and various pathological conditions.

2. Materials and methods

2.1. Peptide synthesis

The amino acid sequence of PRM1 is MARYRCCRSQSRSRYYRQRQRSRRRRRRSCQTRRRAMRCCRPRYRPRCRRH-NH_2.

PRM1 peptides were synthesized by KS-V PEPTIDE (Hefei, China) with a purity of 95%. The purity and identity of the synthesized peptides were assessed using analytical high-performance liquid chromatography (HPLC) (Fig. S1) and mass spectrometry (Fig. S2).

2.2. In vitro CEST MRI of PRM1 solutions

All peptide solutions were prepared at a concentration of 0.733 mM using phosphate-buffered saline (PBS) or distilled water (ddH_2O). The pH of the solutions was adjusted to specific values of 6.5, 6.8, 7.2, and 7.5 by titration with 3 M HCl or NaOH. The prepared samples were then placed in 5 mm nuclear magnetic resonance (NMR) tubes for CEST MRI analysis. MRI measurements were performed using a Bruker 400 MHz wide-bore NMR spectrometer with imaging accessories, equipped with a 25 mm birdcage transmit/receive coil. For CEST MRI, the pulse sequence includes a saturation module followed by a rapid acquisition with relaxation enhancement (RARE) readout, with the following parameters: repetition time/echo time (TR/TE) = 8000/5 ms, RARE factor = 8, slice thickness = 3 mm, matrix size = 128 × 96, B_1 = 0.6–7.2 μT, saturation time (t_{sat}) = 4 s, with saturation offset frequencies ($\Delta\omega$, where ω is the saturation pulse frequency) ranging from −15 to 15 ppm in 0.2-ppm increments, with the water resonance set at 0 ppm. B_0 inhomogeneity was corrected using the water saturation shift referencing (WASSR) method. The CEST signal was quantified using the metric $MTR_{asym} = [S_{sat}(-\Delta\omega)/S_0] - [S_{sat}(\Delta\omega)/S_0]$, where $S_{sat}(-\Delta\omega)$, $S_{sat}(\Delta\omega)$ and S_0 represent the water signal with a saturation frequency offset at $-\Delta\omega$, $\Delta\omega$ and without saturation, respectively [23].

2.3. Plasmid construction

The plasmids pAAV-CAG-EGFP-WPRE-polyA (pAAV-EGFP) and pAAV-CAG-EGFP-P2A-PRM1-WPRE-polyA (pAAV-EGFP-PRM1) were purchased from Brain Case (Shenzhen, China). To facilitate the co-translational proteins PRM1 and EGFP, a P2A self-cleavage sequence was inserted between the two genes.

2.4. In vitro cell studies

293T cells were seeded into T75 flasks and incubated at 37 °C in a 5% CO_2 atmosphere for 24 h to reach approximately 80% confluence. Cells were then transfected with either pAAV-EGFP or pAAV-EGFP-PRM1 plasmids using Lipo8000 transfection reagent (Beyotime, China), following the manufacturer's instructions. After transfection, the cells were incubated for an additional 48 h for MRI analysis. Briefly, cells were treated with trypsin, resuspended in 200 μL of PBS, and centrifuged at 12,000 g for 10 min in 0.2 mL PCR tubes. The supernatant was then prepared for MRI experiments. The MRI sequence used was similar to the one previously described, with the following adjustments: TR/TE = 6000/4.75 ms, number of averages = 1,

slice thickness = 2 mm, FOV = 17 × 17 mm^2, matrix size = 96 × 96, B_1 = 3.6 μT, and t_{sat} = 3 s, with saturation offset frequencies ranging from −4 to 4 ppm in 0.4-ppm increments, with the water resonance set at 0 ppm. B_0 inhomogeneity was corrected using the WASSR method to ensure accurate frequency alignment in the CEST spectra. The cell studies comprised seven replicates and all raw data were processed using MATLAB (R2022a, MathWorks, Natick, MA).

2.5. Production of the rAAVs

The rAAVs were produced in HEK293 cells using the traditional triple-plasmid transfection method [24]. The rAAV-EGFP and rAAV-EGFP-PRM1 vectors were bought from Brain Case (Shenzhen, China).

2.6. Animals

All surgical and experimental procedures were conducted in accordance with the guidelines set by the Animal Care and Use Committee of Innovation Academy for Precision Measurement Science and Technology, Chinese Academy of Sciences (APM21013T). Eight-week-old male C57BL/6 mice were obtained from Beijing Vital River Laboratory Animal Technology Co. Ltd. The mice were housed in a controlled environment with a 12-h light/dark cycle, stable temperature, and humidity, with unrestricted access to food and water.

2.7. Stereotaxic surgery

Five mice were intraperitoneally injected with pentobarbital sodium (50 mg/kg), and positioned in a stereotaxic frame (RWD, China). After exposing the skull, a small hole was drilled to allow the insertion of a glass micropipette (World Precision Instruments, USA). One microliter of purified rAAV solution (5×10^{12} viral genomes/mL in PBS) was stereotaxically injected into the target region, the CPU, using coordinates based on the mouse brain atlas. The coordinates for the CPU were as follows: 0.51 mm anterior to Bregma, ± 2 mm lateral from midline, and 3.3 mm in depth relative to Bregma. The infusion rate was set at 50 nL/min. Upon completion of the injection, the pipette was kept in place for 20 min before being slowly withdrawn. The mice were placed on a warm pad to fully recover from anesthesia before being returned to cages for further observation.

2.8. In vivo CEST MRI

Thirty days after the virus injection, all the five mice were under MRI observation. Anesthesia was induced with 3.5–4.0% isoflurane (RWD, China) then maintained at 1.0–1.5% isoflurane. The respiratory rate was monitored and maintained at approximately 60 breaths per minute. A warm water pad was used to keep the body temperature at approximately 36.5°C. The mouse brain was scanned using a transmit birdcage coil and a receive-only surface coil (20 mm in diameter). For the CEST MRI, a pulse sequence was employed with the following parameters: TR/TE = 6000/4.75 ms, number of averages = 1, slice thickness = 2 mm, FOV = 16 × 14 mm^2, matrix size = 96 × 72, B_1 = 2.4 μT, and t_{sat} = 3 s. Saturation offset frequencies from −4 to 4 ppm in 0.4-ppm increments, with the water resonance set at 0 ppm. B_0 inhomogeneity was corrected using the WASSR method, with a total acquisition time of 5 min. The total scan time for CEST MRI was 12 min and 48 s.

2.9. Statistical analysis

Statistical differences between groups were assessed using Student's t-test, with significance levels set at $*p < 0.05$, $**p < 0.01$ and $***p < 0.001$. The number of independent replicates for each experiment is indicated in the figure captions. All statistical analyses were performed using GraphPad Prism 10 software.

3. Results and discussion

To evaluate the influence of pH levels and saturation field strengths on the CEST contrast of PRM1 solutions, we analyzed a 0.733 mM PRM1 solution. PRM1 exhibited two distinct peaks in the CEST spectra: one corresponding to the amide protons of the protein backbone at a 3.6 ppm offset, the other to the guanidyl protons of the arginine side chain at a 1.5 ppm offset. The CEST signals varied with different pH values due to changes in the exchange rate [25]. Optimal CEST performance was observed within a pH range of 7.2–7.5, which aligns with the physiological range of human brain [26,27]. At pH 7.2, the optimal CEST contrast was noted at 1.5 ppm (Fig. 1a and Fig. S3). The MTR_{asym} spectrum of 0.733 mM PRM1 solution reached a peak of 43%. To identify the optimal saturation power for detecting PRM1, we tested a range of B_1 values. A saturation field of 3.6 μT provided the clearest CEST signal, producing the two characteristic peaks at 3.6 and 1.5 ppm (Fig. 1b), consistent with previously reported data [18]. Based on these findings, we selected 3.6 μT as the saturation power for subsequent *in vitro* experiments evaluating PRM1 as a CEST contrast agent.

To investigate the potential of PRM1 as a CEST contrast agent in cells, we conducted an *in vitro* study using 293T cells. These cells were transfected with a plasmid encoding both EGFP and PRM1, while those transfected with pEGFP alone served as the control group (Fig. 2a). Forty-eight hours post-transfection, the cells were collected for CEST MRI analysis. The Z-

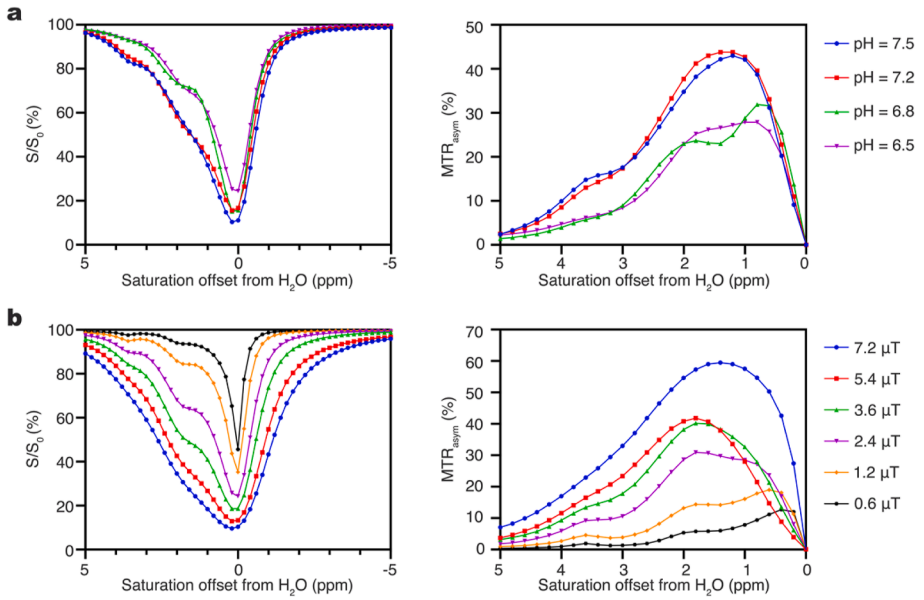

Fig. 1. Z-spectra and MTR_{asym} spectra of PRM1 solutions under different conditions. (a) pH dependence of PRM1 CEST contrast at $B_1 = 3.6$ μT, $T_{sat} = 4$ s; (b) Effect of saturation field strength on PRM1 CEST contrast at pH = 7.2, $T_{sat} = 4$ s.

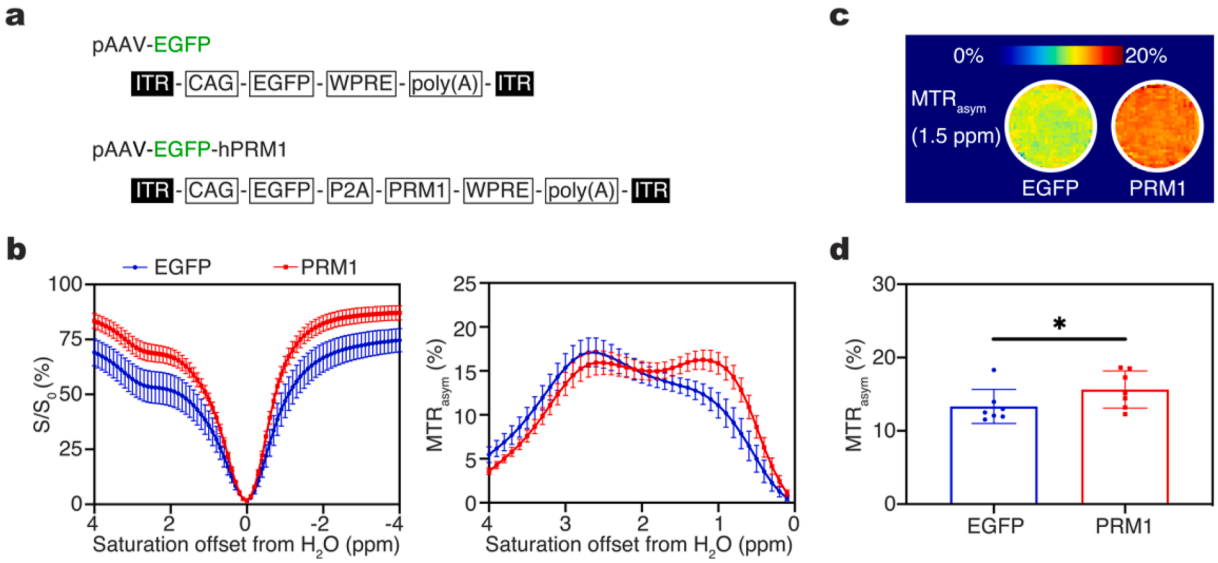

Fig. 2. CEST-MRI of PRM1-expressing 293T cells. (a) Schematic representation of recombinant AAV transfer plasmids encoding the gene of interest (GOI). The GOI, driven by the CAG promoter, is inserted between inverted terminal repeats (ITRs) for ubiquitous protein expression in mammalian cells and gene packaging into the AAV particles. The woodchuck hepatitis virus posttranscriptional regulatory element (WPRE) is included to enhance transgene expression. Plasmid names: pAAV-EGFP and pAAV-EGFP-PRM1. (b) Z-spectra and MTR_{asym} spectra of 293T cells expressing EGFP or EGFP-PRM1. (c) Representative MTR_{asym} maps of 293T cells expressing EGFP or EGFP-PRM1 at a frequency offset of 1.5 ppm. Cells were transfected with AAV transfer plasmids and analyzed using *in vitro* CEST MRI. (d) Mean MTR_{asym} (±SD) at a frequency offset of 1.5 ppm ($n = 7$). CEST data were acquired at 9.4 T, $B_1 = 3.6$ μT, and $T_{sat} = 3$ s.

spectrum and MTR_{asym} spectrum of the transfected cells are shown in Fig. 2b. The MTR_{asym} spectrum around the 1.5 ppm frequency offset for PRM1-expressing cells was remarkably higher than that for the control group. Additionally, a representative MTR_{asym} map at the 1.5 ppm frequency showed a significantly stronger signal in cells with expressed PRM1 compared to those without PRM1 encoding (Fig. 2c–d). These findings suggest that PRM1 is an effective CEST contrast agent in cellular contexts. However, a reduction in CEST contrast was observed *in vivo* compared to the phantom studies, likely due to interference from the nuclear overhauser enhancement (NOE) and magnetization transfer (MT) effects [28,29]. The complex cellular environment, such as phosphorylation or interactions with negatively charged metabolites, may alter the proton exchange behaviors and peptide structure of PRM1, thus affecting its contrast performance [30].

Prior to the *in vivo* studies, we performed optimization experiments using a healthy mouse and a range of B_1 saturation powers (0.5–5.0 μT). Higher saturation powers led to reduced image detail and spectral resolution, particularly affecting brain region differentiation in MTR_{asym} maps (Fig. S4). To optimize both contrast and clarity, 2.4 μT was selected as the optimal saturation power for subsequent *in vivo* studies. To investigate whether CEST MRI could successfully detect PRM1 encoded by rAAV *in vivo*, we stereo tactically injected rAAV-EGFP-PRM1 or rAAV-EGFP into the bilateral CPU regions of the mouse brain (Fig. 3a). The mice were observed under a 9.4 T MRI scanner 30 days post-injection. The brain region injected with rAAV-EGFP-PRM1 exhibited enhanced CEST contrast compared to that of those received rAAV-EGFP treatment, while their T_2-weighted images showed no significant differences (Fig. 3b–c and Fig. S5). The Z-spectrum and MTR_{asym} spectrum of the infected brain demonstrated an enhanced CEST signal at a 1.5 ppm frequency shift in the right CPU ($MTR_{asym} = 4.91\% \pm 0.52\%$), confirming the efficacy of PRM1 for *in vivo* CEST imaging in mouse brains (Fig. 3d–e). In the study that applied amide proton transfer (APT) to assess the CEST value in the human brain, the APT-weighted value was reported as 1.35% ± 0.15% [31]. In contrast, our data showed that the MTR_{asym} value in the right CPU is 3.6 times higher than the APT value, suggesting that PRM1 is a more promising contrast agent compared to endogenous molecules.

This study integrates two promising techniques: MRI reporter-encoding rAAV2 and *in vivo* CEST MRI. By using a Cre-dependent expression cassette in combination with a Cre-transgenic mouse model, this approach promises to enhance the specificity of *in vivo* cell type investigations. Such developments are especially relevant for studying neurodegenerative disorders, such as Parkinson's disease. For example, recent studies have demonstrated a reduction in APT and CEST contrast in the substantia nigra of Parkinson's patients compared to healthy controls [31,32]. However, because this contrast depends on endogenous cellular proteins and peptides, it often encounters sensitivity limitations due to background signal interference. The selective expression of PRM1 in the substantia nigra may provide more precise insights into dopaminergic neurons, offering potential for improved monitoring of Parkinson's disease progression.

The study has some limitations. In complex biological environments, factors such as MT, NOE, and direct water saturation (DS) can affect the accurate quantification of MTR_{asym} signal intensity. To mitigate these effects, multi-pool Lorentz fitting provides an alternative approach for future experiments [33,34]. Additionally, the study utilized stereotactic injection of rAAV vectors into specific brain regions, which is relatively invasive. Non-invasive delivery techniques, such as focused ultrasound blood-brain barrier opening (FUS-BBBO), offer an alternative method for delivering rAAVs directly to targeted brain areas [35,36]. FUS-BBBO has been successfully applied for rAAVs delivery in various animal models. Integrating non-invasive gene delivery with MRI imaging could present a promising strategy for future studies, especially in non-human primates [37].

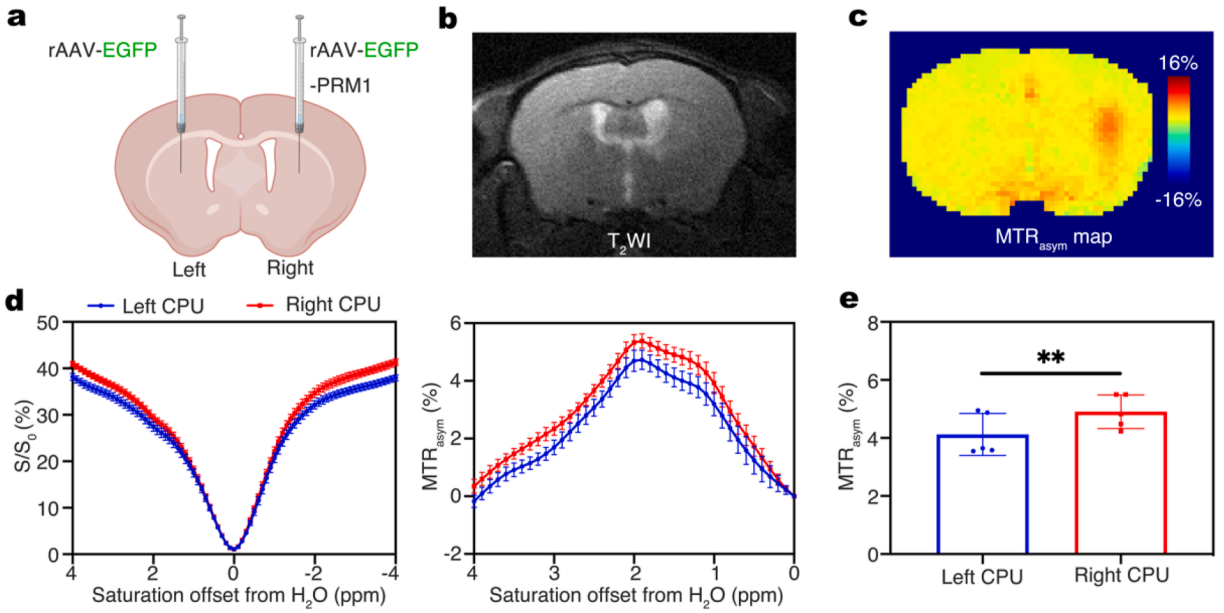

Fig. 3. CEST-MRI of PRM1 in mouse brain. (a) Scheme illustrating a horizontal brain slice with rAAV-EGFP and rAAV-EGFP-PRM1 injections into the bilateral CPU regions. Representative T_2-weighted image (b) and MTR_{asym} map (c) of the mouse brain 30 days post-injection. (d) Z-spectra and MTR_{asym} spectra of left and right CPU regions 30 days post-injection. (e) Mean MTR_{asym} (±SD) at the 1.5 ppm frequency offset for the left and right CPU regions ($n = 5$). CEST data were acquired at 9.4 T, $B_1 = 2.4$ μT, and $T_{sat} = 3$ s.

4. Conclusion

This study presents a novel approach for the *in vivo* detection of brain cells using a CEST contrast agent. By incorporating the PRM1 gene into an rAAV2 vector and employing CEST MRI, we successfully detected transfected brain cells in the CPU region. This method provides valuable insights into dynamic brain changes under both physiological and pathological conditions, with promising applications for advanced analysis in larger animals, including non-human primates.

CRediT authorship contribution statement

Kairu Xie: Writing – original draft, Visualization, Validation, Methodology, Investigation, Formal analysis, Data curation. **Yaping Yuan:** Methodology, Investigation, Formal analysis. **Mou Jiang:** Validation, Software, Methodology, Investigation. **Daiqin Chen:** Writing – original draft, Methodology, Investigation. **Shizhen Chen:** Writing – review & editing, Project administration, Methodology, Investigation, Funding acquisition, Conceptualization. **Xin Zhou:** Writing – review & editing, Methodology, Investigation, Formal analysis, Conceptualization.

Declaration of competing interest

The authors declare the following financial interests/personal relationships which may be considered as potential competing interests: Xin Zhou is an editorial board member of *Magnetic Resonance Letters* but was not involved in the editorial review or the decision to publish this article.

Acknowledgement

This work was financially supported by the National Natural Science Foundation of China (82127802, 22374157); Strategic Priority Research Program, CAS (XDB0540000, XDC0170000); CAS Youth Interdisciplinary Team (JCTD-2022-13). In addition, Xin Zhou acknowledges the support from the Tencent Foundation through the XPLORER PRIZE.

Appendix A. Supplementary data

Supplementary data to this article can be found online at https://doi.org/10.1016/j.mrl.2025.200222.

References

[1] L. Pini, M. Pievani, M. Bocchetta, et al., Brain atrophy in Alzheimer's disease and aging, Ageing Res. Rev. 30 (2016) 25–48.
[2] G. Frisoni, N. Fox, C. Jack, et al., The clinical use of structural mri in Alzheimer disease, Nat. Rev. Neurol. 6 (2010) 67–77.
[3] R. Stefania, L. Palagi, E. Di Gregorio, et al., Seeking for innovation with magnetic resonance imaging paramagnetic contrast agents: relaxation enhancement via weak and dynamic electrostatic interactions with positively charged groups on endogenous macromolecules, J. Am. Chem. Soc. 146 (2023) 134–144.
[4] S. Dumoulin, A. Fracasso, W. van der Zwaag, et al., Ultra-high field mri: advancing systems neuroscience towards mesoscopic human brain function, Neuroimage 168 (2018) 345–357.
[5] D. Foster, J. Larsen, Polymeric metal contrast agents for T1-weighted magnetic resonance imaging of the brain, ACS Biomater. Sci. Eng. 9 (2023) 1224–1242.
[6] E. Debroye, T. Parac-Vogt, Towards polymetallic lanthanide complexes as dual contrast agents for magnetic resonance and optical imaging, Chem. Soc. Rev. 43 (2014) 8178–8192.
[7] Q. Meng, M. Wu, Z. Shang, et al., Responsive gadolinium(Iii) complex-based small molecule magnetic resonance imaging probes: design, mechanism and application, Coord. Chem. Rev. 457 (2022), https://doi.org/10.1016/j.ccr.2021.214398.
[8] T. Kanda, H. Oba, K. Toyoda, et al., Brain gadolinium deposition after administration of gadolinium-based contrast agents, Jpn. J. Radiol. 34 (2016) 3–9.
[9] D. Stojanov, A. Aracki-Trenkic, D. Benedeto-Stojanov, Gadolinium deposition within the dentate nucleus and globus pallidus after repeated administrations of gadolinium-based contrast agents-current status, Neuroradiology 58 (2016) 433–441.
[10] K.M. Ward, A.H. Aletras, R.S. Balaban, A new class of contrast agents for mri based on proton chemical exchange dependent saturation transfer (cest), J. Magn. Reson. 143 (2000) 79–87.
[11] P.C.M. van Zijl, N.N. Yadav, Chemical exchange saturation transfer (cest): what is in a name and what Isn't? Magn. Reson. Med. 65 (2011) 927–948.
[12] K.W.Y. Chan, M.T. McMahon, Y. Kato, et al., Natural D-glucose as a biodegradable mri contrast agent for detecting cancer, Magn. Reson. Med. 68 (2012) 1764–1773.
[13] S. Walker-Samuel, R. Ramasawmy, F. Torrealdea, et al., *In vivo* imaging of glucose uptake and metabolism in tumors, Nat. Med. 19 (2013) 1067–1072.
[14] M. Haris, K. Cai, A. Singh, et al., *In vivo* mapping of brain myo-inositol, Neuroimage 54 (2011) 2079–2085.
[15] F. Kogan, A. Singh, C. Debrosse, et al., Imaging of glutamate in the spinal cord using glucest, Neuroimage 77 (2013) 262–267.
[16] M. Haris, R. Nanga, A. Singh, et al., Exchange rates of creatine kinase metabolites: feasibility of imaging creatine by chemical exchange saturation transfer Mri, NMR Biomed. 25 (2012) 1305–1309.
[17] F. Kogan, M. Haris, C. Debrosse, et al., *In vivo* chemical exchange saturation transfer imaging of creatine (Crcest) in Skeletal Muscle at 3t, J. Magn. Reson. Imag. 40 (2014) 596–602.
[18] A. Bar-Shir, G.S. Liu, K.W.Y. Chan, et al., Human protamine-1 as an Mri reporter gene based on chemical exchange, ACS Chem. Biol. 9 (2014) 134–138.
[19] M. Kaplitt, A. Feigin, C. Tang, et al., Safety and tolerability of gene therapy with an adeno-associated virus (Aav) borne gad gene for Parkinson's disease: an open label, phase I trial, Lancet 369 (2007) 2097–2105.
[20] A. Cai, N. Zheng, J. Garth, et al., Longitudinal neural connection detection using a ferritin-encoding adeno-associated virus vector and *in vivo* Mri method, Hum. Brain Mapp. 42 (2021) 5010–5022.
[21] N. Zheng, P. Su, Y. Liu, et al., Detection of neural Connections with Ex vivo Mri using a Ferritin-encoding trans-synaptic virus, Neuroimage 197 (2019) 133–142.

[22] N. Zheng, M. Li, Y. Wu, et al., A novel Technology for *in vivo* detection of cell type-specific neural connection with Aqp1-encoding Raav2-Retro vector and metal-free Mri, Neuroimage 258 (2022), https://doi.org/10.1016/j.neuroimage.2022.119402.
[23] X. Zhang, Y. Yuan, S. Li, et al., Free-base porphyrins as cest Mri contrast agents with highly upfield shifted labile protons, Magn. Reson. Med. 82 (2019) 577–585.
[24] Y. Wu, L. Jiang, H. Geng, et al., A recombinant baculovirus efficiently generates recombinant adeno-associated virus vectors in cultured insect cells and larvae, Mol.Ther.-Methods Clin. Dev. 10 (2018) 38–47.
[25] D. Longo, W. Dastrù, G. Digilio, et al., Iopamidol as a responsive Mri-chemical exchange saturation transfer contrast agent for Ph mapping of kidneys: *in vivo* studies in mice at 7 T, Magn. Reson. Med. 65 (2011) 202–211.
[26] P. Orlowski, M. Chappell, C.S. Park, et al., Modelling of Ph dynamics in brain cells after stroke, Interface Focus 1 (2011) 408–416.
[27] J.R. Casey, S. Grinstein, J. Orlowski, Sensors and regulators of intracellular Ph, Nat. Rev. Mol. Cell Biol. 11 (2010) 50–61.
[28] H. Zhang, H. Kang, X. Zhao, et al., Amide proton transfer (Apt) Mr imaging and magnetization transfer (Mt) Mr imaging of pediatric brain development, Eur. Radiol. 26 (2016) 3368–3376.
[29] K. Cai, A. Singh, H. Poptani, et al., Cest signal at 2ppm (Cest@2ppm) from Z-spectral fitting correlates with creatine distribution in brain tumor, NMR Biomed. 28 (2015) 1–8.
[30] N. Oskolkov, A. Bar-Shir, K.W.Y. Chan, et al., Biophysical characterization of human protamine-1 as a responsive cest mr contrast agent, ACS Macro Lett. 4 (2015) 34–38.
[31] C.M. Li, M. Chen, X.N. Zhao, et al., Chemical exchange saturation transfer Mri signal loss of the substantia nigra as an imaging biomarker to evaluate the diagnosis and serverity of Parkinson's disease, Front. Neurosci. 11 (2017), https://doi.org/10.3389/fnins.2017.00489.
[32] C.M. Li, S. Peng, R. Wang, et al., Chemical exchange saturation transfer Mr imaging of Parkinson's disease at 3 Tesla, Eur. Radiol. 24 (2014) 2631–2639.
[33] Z. Dai, S. Kalra, D. Mah, et al., Amide signal intensities may Be reduced in the motor cortex and the corticospinal tract of Als patients, Eur. Radiol. 31 (2021) 1401–1409.
[34] Y. Wu, I. Zhou, D. Lu, et al., Ph-sensitive amide proton transfer effect dominates the magnetization transfer asymmetry contrast during acute ischemiaquantification of multipool contribution to *in vivo* cest Mri, Magn. Reson. Med. 79 (2018) 1602–1608.
[35] A. Alonso, E. Reinz, B. Leuchs, et al., Focal delivery of Aav2/1-transgenes into the rat brain by localized ultrasound-induced Bbb opening, Mol. Ther.-Nucl. Acids 2 (2013), https://doi.org/10.1038/mtna.2012.64.
[36] S. Wang, O. Olumolade, T. Sun, et al., Noninvasive, neuron-specific gene therapy can Be facilitated by focused ultrasound and recombinant adeno-associated virus, Gene Ther. 22 (2015) 104–110.
[37] A. Carpentier, M. Canney, A. Vignot, et al., Clinical trial of blood-brain barrier disruption by pulsed ultrasound, Sci. Transl. Med. 8 (2016), https://doi.org/10.1126/scitranslmed.aaf6086.

Xin Zhou received Ph.D. degree from Wuhan Institute of Physics and Mathematics, Chinese Academy of Sciences in 2004. After his postdoctoral research periods in Harvard University (2005–2007) and research fellow experience in University of California Berkeley (2007–2009), he joined Wuhan Institute of Physics and Mathematics, Chinese Academy of Sciences. The research interests of his group are mainly focused on the development of novel methodology and techniques of NMR. Group homepage: http://zhou.apm.ac.cn/.

Shizhen Chen received her Ph.D. degree in Analytical Chemistry from Central China Normal University in 2011. From 2011 to 2013, she completed postdoctoral training at the Wuhan Institute of Physics and Mathematics, Chinese Academy of Sciences, where she now serves as a professor. Her work focuses on multi-nuclear magnetic resonance molecular imaging.

Kairu Xie received her M.D. from the Tongji Medical College at Huazhong University of Science and Technology (HUST), Wuhan, in 2018. She is currently pursuing a Ph.D. at the Wuhan National Laboratory for Optoelectronics, HUST. Her research focuses on nucleic acid delivery vectors and magnetic resonance imaging.